The final publication is available at Springer via https://doi.org/10.1007/s12273-020-0751-x

Evaluating the impact of thermostat control strategies on the energy flexibility of residential buildings for space heating

Kun Zhang, Michaël Kummert

Department of Mechanical Engineering, Polytechnique Montreal, Montreal, Canada

Abstract

Buildings can be operated in an energy-flexible manner while respecting occupant thermal comfort. This energy flexibility of building operations, both in time and quantity, can be harnessed by the electrical grid for load balancing. In the context of smart grid and intelligent buildings, the concept of energy flexibility in buildings broadens the existing demand management thinking from the top-down one-way control to two-way communications. This paper, extending studies on thermostat controls of heating and air conditioning systems for demand response, evaluates the impact of different control schemes on the energy flexibility of residential buildings. Two control strategies, Model Predictive Control (MPC) and Rule-Based Control (RBC), are investigated for a space heating system using co-simulation studies. Four indicators are introduced and adapted from the literature to assess the control performances of the strategies. Simulation results show that different flexibility indicators favour different control strategies in this case study. For demand response events of four hours, the MPC strategy presents two to three times of flexible energy than that of RBC. MPC also delivers 20% more of maximum power reduction during the events against RBC. The RBC strategy, on the other hand, is twice of MPC for flexible energy efficiency. This evaluation work can be beneficial to guide the control system design of new buildings or control retrofits of existing buildings that consider better grid-building interactions for the future.

Keywords: energy flexibility, MPC, grid-building interaction, demand response

Introduction

Demand Side Management (DSM) has been considered as a feasible solution by the electrical utility to reduce its peak power demand. Comparing with operating reserved peak plants or purchasing power from other resources in the period of power scarcity, DSM has been shown to be more cost-effective and reduces carbon dioxide emissions (Davito et al. 2010). When the grid is integrated with renewable energy sources (RES), DSM can be more instrumental for the grid to balance its supply and demand. The variability of renewables and their dependence on climate conditions add challenges to the grid operation.

Buildings, due to their high demand for electrical power, could be managed as a key asset for DSM (Li et al. 2017). Among the DSM approaches, various Demand Response (DR) programs have been piloted and put into practices during the past decades, for instance, for load shifting (Palensky & Dietrich 2011) and load shedding (Lanzisera et al. 2015).

DR programs have been evolving through time in response to technology advancement and new challenges. As the understanding grows for the smart grid and intelligent buildings, new ideas are required to fit into the new context. The terminology of energy flexibility is a more general term than the existing ones used in the DSM communities, such as demand limiting, load shedding, shifting and shaping (Alstone et al., 2017). Instead of viewing the demand from the top-down perspective, the term energy flexibility includes considerations of two-way communications and interactions between the grid and buildings. In such a way, the buildings are regarded not merely as consumers but prosumers (Karnouskos et al. 2012).

Three types of systems in or around buildings contribute to energy flexibility: energy storage systems, Distributed Energy Resources (DERs) or alternative fuels supplying to the buildings. The storage systems include the thermal mass of buildings, Phase Change Materials (PCM) applied to the building envelope or thermal storage, domestic water tanks, ice storage and battery. DERs incorporate building integrated photovoltaic panels, solar thermal collectors and wind turbines. The last type of flexibility is through the fuel switch. For instance, gas or oil, if existing, can sustain the building's thermal demand during peak electricity prices.

A more formal yet broad definition states that the energy flexibility of a building is "the ability to manage its demand and (energy) generation according to its local climate conditions, user needs and energy network requirements" by the Annex 67 of Energy in Buildings and Communities

(EBC), International Energy Agency (IEA) (Jensen et al. 2017). It is worth noting that the Annex 67 does not address the very short timescale storage in seconds for frequency stabilization (Ulbig et al. 2014). The flexibility in the time dimension discussed in the Annex and this paper is on the scale of hours, which is consistent with the diurnal peak durations of the grid. Like the energy performance certificate, the flexibility can be added as an extra label on buildings. For a broader context and application of energy flexible buildings, the Annex 67 position paper provides more details (Jensen et al. 2017).

Sequential to the Annex 67 project, several other national and international projects were launched to address similar issues. In 2017, the European Energy Performance of Building Directive (EPBD) initiated a project called "Smart Readiness Indicator (SRI)" for buildings. In the SRI system, energy flexibility is adopted as one of the eight indicators to assess the smart readiness of a building. In 2018, a project called GridOptimal was launched by the New Building Institute and the United States Green Building Council (USGBC). Similar to the USGBC Leadership in Energy and Environmental Design (LEED) program, the project aims to develop a new rating system to standardize metrics and provide guidelines to evaluate levels of interactions between the grid and buildings (New Buildings Institute, 2018). In 2019, the U.S. Department of Energy started a multi-laboratory collaboration on the project "Grid-interactive efficient buildings (GEB)", which explores to combine energy efficiency measures of buildings with the extra capabilities of grid interactions to provide ancillary services to the grid (Nuekomm et al. 2019).

The initiations of those projects indicate that it is still in the developing process of a standardized framework to quantify and evaluate the building energy flexibility. Among the previous studies, Finck et al. (2018) had a thorough review of earlier DR studies and summarized the Key Performance Indicators (KPIs) proposed in the literature which could be useful to quantify energy flexibility. The proposed KPIs were mostly for their specific case studies, such as for PV or thermal storage systems. Yin et al., (2016) studied the potential of global setpoint temperature adjustment of residential and commercial buildings for DR applications. The DR potential was defined as the difference between baseline and DR load divided by the baseline load. The DR potential was investigated on two levels: individual customer and substation. De Coninck & Helsen (2016) studied the energy flexibility of a commercial building by optimizing the operation of heat pumps and hot water tanks. The objective was to minimize energy cost using spot market electricity price

with around 2 °C of thermal comfort range. (Kathirgamanathan et al., 2020) investigated three different KPI definitions and applied them to three different buildings.

Two vintages of residential buildings with two types of space heating systems were studied for their energy flexibility through simulation studies by Le Dréau & Heiselberg (2016). The thermal mass was viewed as a thermal battery, where the amount of thermal energy charged and discharged by the building during DR events was regarded as the energy flexibility indicators. A similar approach was adopted in (Reynders et al. 2015, 2017), where two types of dwellings at 4 different construction periods were simulated. Two performance indicators were used: flexibility capacity and storage efficiency. These two teams regarded the building thermal mass as a thermal storage system and the indicators are in the unit of thermal energy, not electrical energy. (Barzegar et. al. 2018) studied the energy flexibility of building-integrated solar photovoltaic and battery system and adopted indicators more specific to the electrical system.

Among the existing studies of energy flexibility, the focus was mostly on the impact of building envelopes or various types of Heating, Cooling and Air Conditioning (HVAC) systems. It can be argued that control strategies of HVAC systems could also contribute to the potential of building flexibility. Furthermore, advanced control strategies (e.g., MPC) would probably present more potential than a simple Rule-Based Control (RBC) that was adopted in most studies.

The objective of this work is to evaluate the impact of HVAC control strategies on building energy flexibility. Two control strategies RBC and MPC, as well as two MPC configurations, are evaluated using a set of KPIs. The RBC strategy represents the current practice, which is a stable and low-cost implementation. MPC represents a future advanced control scheme, which still suffers high cost and uncertainty in real-world applications. The two MPC methods and the RBC method are then compared against each other using the defined KPIs. Note that the RBC strategy considered in this study only reacts to DR events and does not include any pre-conditioning algorithm, which leads to disadvantages compared with MPC for certain indicators.

The contribution of this paper includes a detailed evaluation of the impact of HVAC control strategies on energy flexibility, which complements the existing work on the evaluation of the impact of building envelopes and HVAC system types. The contribution also includes a detailed comparison of control strategies. In general, evaluation of different control methods could inform engineers on whether advanced control would deliver a better outcome for energy flexibility than

simple controls, and how much better if possible. If the advanced control does provide benefits for the smart grid or gain points in the rating of building smartness, the evaluation analysis could be essential to guide control system design or retrofit. In addition, this paper has extended the existing KPIs to include the maximum flexible power and discussed this indicator with results.

The paper is structured in the following sections. Section *Methodology* explains the methods of MPC and RBC in this study and introduces the KPIs adapted from existing studies. It follows an illustration of building and HVAC system modelling and how the controls are implemented. The two configurations of MPC modelling are detailed. Section *Results* presents the comparison and analysis of simulation results. The paper concludes with discussions and recommendations.

Methodology

Flexibility definition

In this paper, the building energy flexibility is categorized into two types of scenarios: upward flexibility, and downward flexibility.

The upward flexibility (also known as positive flexibility) is the capability of buildings to consume more energy when the grid confronts more power supply than its demand. This situation happens more often when RES is integrated into the grid, where the renewables may overload the grid during certain periods. An example of this situation is the “duck curve” of the Californian utility California Independent System Operator because of the solar generation (California ISO, 2017).

Contrary to the upward flexibility, the downward flexibility (also known as negative flexibility) is the capability of buildings to consume less energy when the grid experiences less power supply than its demand. This scenario is similar to conventional peak load reduction.

Essentially, the conventional grid services such as demand limiting, load shedding, load shifting, load tracking can be regarded as either downward flexibility, or a combination of downward and upward flexibility at a given time period.

Metrics

Four indicators are introduced in this paper to quantify energy flexibility. A conceptual building demand shape in response to a downward flexibility event is presented in Figure 1. The flexibility

event occurs from 8:00 to 10:00, where E_f denotes the amount of flexible energy in kWh; E_{rb} rebound energy in kWh; P_{fmax} maximum flexible power in kW and t_{dr} event duration in hours. The pre-bound energy use before the event depicts the MPC anticipation effect assuming that MPC knows the occurrence of the event in advance. In a reactive control scheme like RBC, the energy rebound happens most likely after the event.

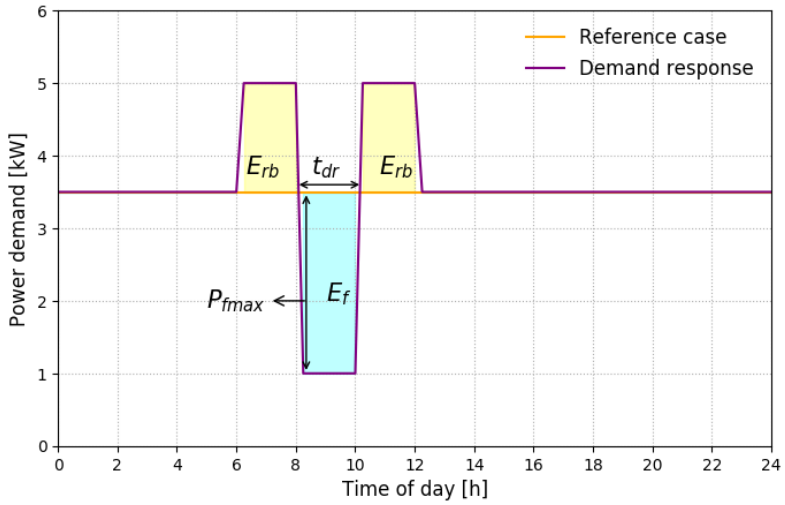

Figure 1: A building demand profile responding to a downward flexibility event;

E_f: flexible energy (kWh); E_{rb}: rebound energy (kWh); P_{fmax}: maximum flexible power (kW); t_{dr}: event duration (h). The pre-bound depicts the MPC anticipation effect.

Flexible energy E_f

The flexible energy quantifies the energy change against the reference scenario, either downward or upward, during the DR event. The cyan shaded area shown in Figure 1 indicates the downward flexible energy amount. A formal equation to calculate the flexible energy can be written as Eq. (1), where P_{dr} is the power in the case of demand response or flexibility event (the purple curve in Figure 1) and P_{ref} is the power in the reference case (the orange curve in Figure 1).

$$\boldsymbol{E_f} = \int_0^{t_{dr}} (P_{dr} - P_{ref}) dt \tag{1}$$

Rebound energy E_{rb}

The energy surge before or after the flexibility event, either positively or negatively, is called rebound energy. The total rebound energy E_{rb} is defined as the equation below.

$$\boldsymbol{E_{rb}} = \int_{t_{-\infty}}^{t_{dr}} (P_{dr} - P_{ref})dt + \int_{t_{dr}}^{t_{\infty}} (P_{dr} - P_{ref})dt \quad (2)$$

The first term of Eq. (2) indicates the extra energy use before the DR event; the second term denotes the additional energy use after the event. The two infinity signs $-\infty$ and ∞ denote the pre-bound and rebound horizons. They can be several hours or longer depending on the studied systems. In this study, $\pm$ 48 hours are used for the computation of the rebound energy because it is confirmed that the simulated building shows no rebound nor pre-bound longer than 48 hours.

Flexible energy efficiency $\boldsymbol{\eta}$

The flexible energy efficiency, based on the idea of the coefficient of performance, is introduced to evaluate the flexibility performance in terms of energy quantity.

$$\boldsymbol{\eta} = \left|\frac{E_f}{E_{rb}}\right| \times 100\% \quad (3)$$

Maximum flexible power $\boldsymbol{P_{fmax}}$

The maximum flexible power denotes the maximum amount of power increase or decrease during an event comparing to the baseline. For the grid, the maximum flexible power indicates the potential power reduction or increase that the consumer can achieve during the events. It can also be an important indicator for consumers if demand charges exist. Given that a rebound effect can happen during an event, two equations are defined separately for upward and downward scenarios as shown in Eq. (4).

$$\boldsymbol{P_{fmax}} = \begin{cases} \max\limits_{t_{dr}} (P_{dr} - P_{ref}) \\ \max\limits_{t_{dr}} (P_{ref} - P_{dr}) \end{cases} \quad \text{for} \begin{matrix} \text{upward} \\ \text{downward} \end{matrix} \quad (4)$$

Controls comparison

The control strategies assessed for energy flexibility in this study are MPC and RBC for the HVAC system. Figure 2 shows the simulation framework of those two control strategies. The real-world building is simulated as a virtual system, represented by a high-fidelity model created in TRNSYS.

The whole building model was calibrated using measurements. Section *Modelling and implementation* illustrates the modelling details of this study.

The two controls are executed on the same virtual system. The control inputs of both methods are setpoint temperatures for the building zones and the feedback signals are "measured" zone air temperatures. The MPC strategy incorporates two modelling approaches: one uses the same detailed model as the virtual system; the other uses a reduced-order model constructed in MATLAB. The first MPC method using detailed modelling is relatively straightforward to configure for building engineers. If models in Building Performance Simulation (BPS) tools are already available, this configuration of co-simulations can be fairly convenient. The second configuration takes more time to identify suitable parametric models. It is, however, more computationally efficient and more suitable for deployment in the hardware for real-time control.

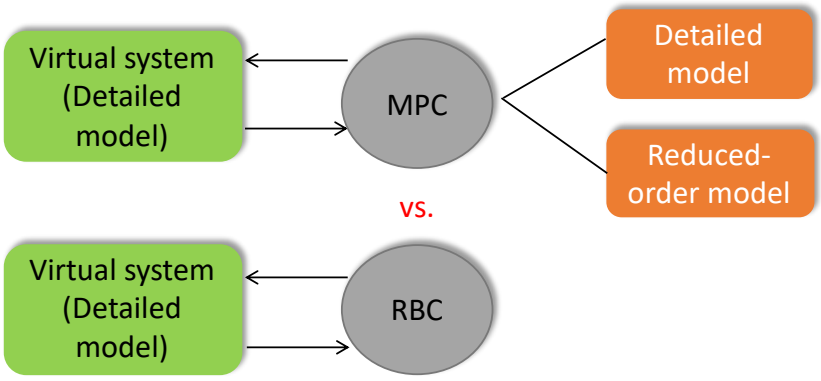

Figure 2: Comparison of control strategies for energy flexibility: MPC vs. RBC

The model predictive control framework

The MPC method implemented in this work is on the supervisory level. The additional MPC controller does not replace room-level thermostats; it instead interacts with the local thermostats. Figure 3 shows the block diagram of the implementation, where the virtual system is the TRNSYS model as shown in Figure 2. The MPC controller, using predictions and forecast from its internal model, computes a time series of optimal setpoints within the control horizon. It then sends the optimal setpoint at the next sampling interval to the room thermostats. The thermostats, using their control logic, determine whether to request a response from the serving HVAC system or not. In this implementation, the thermostats are modelled as an idealized controller in TRNSYS.

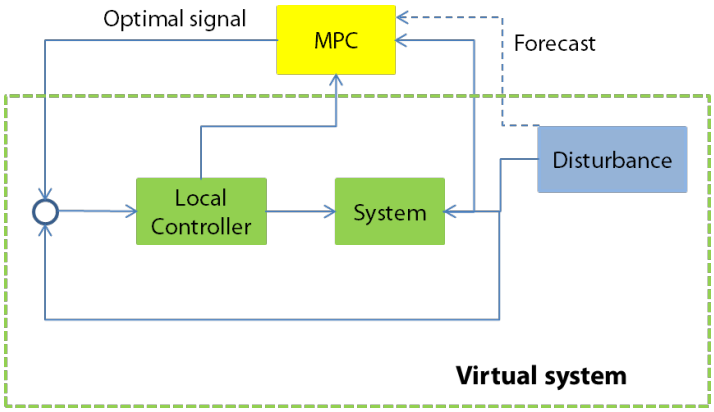

Figure 3: Supervisory model predictive control of the HVAC system

The objective of MPC is to maximize energy flexibility during DR events subject to thermal comfort constraints. Maximizing energy flexibility means decreasing energy use during the downward flexibility event or increasing energy use during upward flexibility. This objective may or may not increase flexibility efficiency. The formulation of the objective function and the MPC implementation are detailed in Section *Modelling and implementation*.

Rule-based control strategy

The RBC strategy reacts to the DR event when it occurs by modulating the setpoint temperature. This means that the RBC strategy does not know the occurrence of events ahead and does not prepare the building for the events through pre-heating or pre-cooling. The implemented RBC setpoint control in this study is to:

- decrease the reference setpoint in the downward flexibility event;
- increase the reference setpoint in the upward flexibility event.

The magnitude of setpoint change is subject to varying comfort constraints and reference setpoint. The RBC strategy assumes that the setpoint always goes to the comfort constraint boundary within one timestep (15 minutes in our case). It is also assumed that the setpoint (not necessarily the zone temperatures) goes back to the reference level until the end of the event within one timestep. The RBC strategy is implemented as an idealized controller in TRNSYS; i.e., no PID controller is implemented.

For the sake of simplicity, only downward flexibility results were included and discussed in this paper for both RBC and MPC. Results for upward flexibility using the RBC method can be found in (Zhang & Kummert, 2018).

Modelling and implementation

Building model

The selected residential building for the study is the twin houses at the Canadian Centre for Housing Technology (CCHT) (see Figure 4 for the picture of the houses). The layout of the houses is to represent typical single-family dwellings in Canada, which include three stories: a basement, a main floor on the ground, a second floor, an attic and a garage. The main floor serves as a living space including a living room and a kitchen. The second floor serves as sleeping rooms. The total floor area of the houses is about 283 m^2. The construction properties were based on the Canadian standard R-2000 (Natural Resources Canada, 2012). The design value of the wall insulation was 3.5 m^2K/W and the windows were coated with a low-emissivity film and filled with argon. The design value of the infiltration rate was 1.5 per hour at 50 Pa. (Manning, Swinton, Szadkowski, Gusdorf, & Ruest, 2007).

The detailed building model was constructed in TRNSYS and calibrated using historical measurements. The whole building model and components, as well as calibration results, are detailed in (Zhang, 2018). Three conditioned zones were included in the model, i.e., basement, main floor and the second floor. The attic and garage were modelled as unconditioned zones. The present paper only reports the controls of the space heating system. The heating system is electric baseboard, which is a common practice in the province of Quebec in Canada. The zone controller was modelled as an idealized thermostatic control. Each conditioned zone is controlled independently with its own thermostat.

Figure 4: The twin houses at the Canadian Centre for Housing Technology for comparative studies

The second column of Table 1 shows the assumption of the occupancy schedule of the basement and main floor. Note that the sleeping floor is not actively controlled, which is set as a constant reference temperature setpoint. The actively controlled floor area is about 180m^2. The second column shows the assumption of DR events occurrence, each of which is assumed to last four hours.

Table 1: Demand response and occupancy schedule

	Occupancy	**DR event**
Morning	06:30~08:00	05:30~09:30
Afternoon	16:30~22:00	16:30~20:30

Comfort constraint

By controlling the HVAC system, the energy flexibility is possible due to the thermal storage in the building mass, if no active thermal storage system existing in the building. The thermal mass is a passive attribute of buildings, but the thermal storage can be indirectly controlled via the activation and deactivation of the HVAC system. The thermal comfort thus should be an important boundary condition for energy flexibility.

In this study, it is assumed that the reference setpoint of the building for each floor is constantly 21 °C. The occupancy schedule impacts the thermal comfort range: a larger thermal comfort band

is assumed for the unoccupied period and a narrower comfort band for the occupied period as shown in Table 2.

Table 2: Thermal comfort constraints for heating and reference heating setpoint

	Occupied	**Unoccupied**
Comfort constraint	20 ~ 23 °C	18 ~ 25 °C
Reference setpoint	21 °C	

MPC with detailed modelling

In the MPC configuration with detailed modelling, the controller model uses the same model as the virtual system as shown in Figure 2. In other words, there is no modelling error in this MPC formulation.

Objective

The objective function is defined as in Eq. (5) to minimize the total energy use while satisfying the defined thermal comfort. The term on the left-hand side denotes the total electricity cost over the control horizon with U_k indicating the power demand at time k and R_k the Time-Of-Use (TOU) electricity price. The price during the events is twice of that out of the events. The same price signal is used in both MPC methods. The term on the right-hand side denotes the penalty cost of zone temperature deviations from the comfort levels. T_k represents zone temperatures at time k and $T_{ub,k}$ and $T_{lb,k}$ represents the upper bound and lower bound of the thermal comfort respectively. μ denotes a scaling coefficient so that the penalty cost is in the same dimension as the energy cost. The penalty function is evaluated as zero when the room temperature is between the defined comfort range. When the zone temperatures are outside of the comfort bounds, the penalty function becomes more dominant in the overall objective function. The final value of μ is obtained through trial and error based on the performance of the optimization algorithm and the acceptable tolerance of violation of thermal comforts is assumed to be 0.5 °C.

$$J = \sum \left(R_k U_k + \mu \left(\max(0, T_k - T_{ub,k}) + \max(0, T_{lb,k} - T_k) \right) \right) \quad (5)$$

Implementation

The MPC framework is implemented using TRNSYS-GenOpt co-simulation. GenOpt is a generic optimization program developed primarily for building systems. It provides users with the freedom

to define their own forms of objective functions or penalty functions and does not require derivatives of the objective functions. Figure 5 presents how TRNSYS and GenOpt interact with each other in the optimal control process (Quintana & Kummert, 2015).

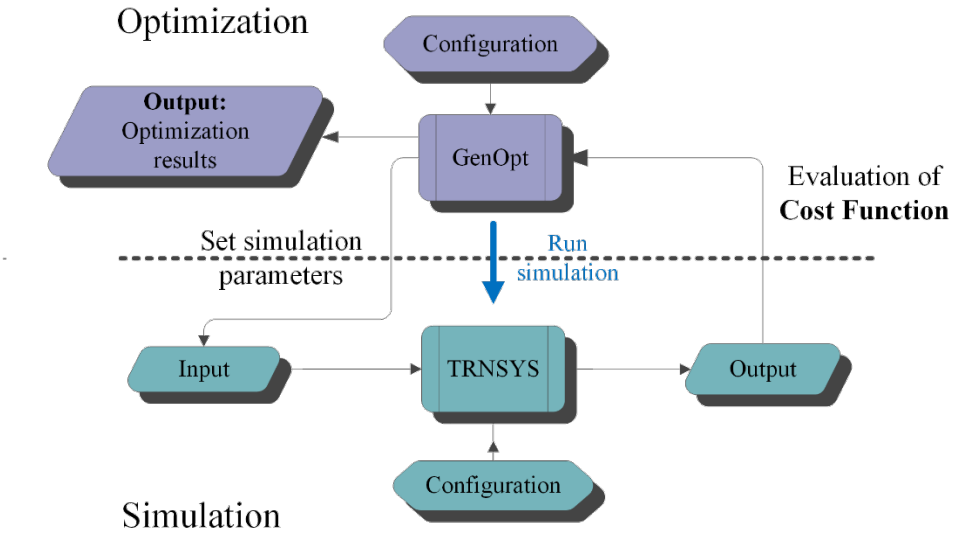

Figure 5: Co-simulation framework between TRNSYS and GenOpt for model predictive control

Before the initialization of the optimization process, template TRNSYS files need to be created listing optimization parameters, inputs and outputs. During the iterations, GenOpt tries different values for the optimization parameters within the defined search space and mesh points and computes the objective function for each parameter combination. The optimization terminates with the minimum objective function value, where GenOpt, however, does not guarantee a global minimum.

This study employed the "Hybrid Generalized Pattern Search (GPS) Algorithm with Particle Swarm Optimization (PSO)" from the algorithm library. This hybrid algorithm performs optimization in two steps. First, it launches the PSO algorithm for user-defined generations (10 generations in this study); Once the PSO has finished successfully, the hybrid algorithm then starts the second GPS algorithm based on the results obtained from the PSO algorithm. When the objective function does not decrease on defined reduced mesh points, the hybrid algorithm then terminates the optimization.

The co-simulation configuration is rather straightforward. However, because of the derivative-free optimization algorithm in GenOpt, it is fairly time-consuming for the tool to converge to an optimal

solution. Only 24 hours of optimization with a 15-minute time step was therefore used in this study.

The configuration and implementation of the co-simulation framework are described briefly in the following steps.

1. Determine control objectives and parameters/variables, as well as constraints of the investigated system such as physical constraints and system operation bounds;
2. Formulate the objective function in equations; if needed, add penalty function in the objective function to consider violation costs of constraints;
3. Model the studied system in one of the BPS tools and simulate for a year with the baseline control strategy;
4. Prepare configuration files for GenOpt and the selected BPS tools for initial testing runs to debug syntax errors;
5. Verify initial optimization results to ensure the algorithm converges to reasonable solutions;
6. Conduct formal optimization-simulation runs and post-process optimization results;
7. Compute performance indicators and evaluate the optimal control strategy against the baseline case.

MPC with the reduced-order model

In the MPC configuration with the reduced-order model, the controller model is a grey-box model of the building. It is formulated in the linear state-space structure in MATLAB. Then co-simulation between TRNSYS and MATLAB is configured using the TRNSYS Type 155.

Reduced-order model formulation

The Resistance-Capacitance (RC) network was used to represent the building model in the reduced-order modelling case, where one resistance and one capacitance were employed to model one thermal zone. This choice was made based on studies in (Mathews et al., 1994; Bacher & Madsen, 2011; Rodríguez Jara et al., 2016). A network of six resistances and three capacitances,

based on this lumped capacitance and resistance assumption, was drawn for the studied house. Figure 6 shows the thermal network diagram.

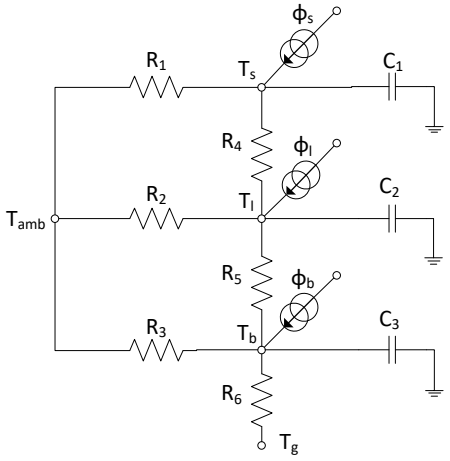

Figure 6: RC network model structure of the CCHT houses

In the network, one conditioned zone is denoted by one node with T_s, T_l and T_b denoting the zone temperatures of the three zones respectively: sleeping room (the second floor), living room (the main floor) and basement. ϕ_s, ϕ_l and ϕ_b represent the total heat added in each zone, which includes the controlled heating flowrate, internal gains and solar gains. The outdoor dry-bulb temperature and ground temperature are inputs of the model, shown by a node in the diagram. Every two nodes are connected with one thermal resistance.

Based on the RC network, a first-order differential equation can be written for each zone. The overall model is therefore a 3rd order system. The differential equations can be further formulated using a vectorized continuous state-space equation as shown in Eq. (6). Given that the output variables are the same as the state variables, denoted by the vector $x = [T_s \quad T_l \quad T_b]^T$, the output equation can be excluded. To more conveniently formulate the objective function, as shown in Eq. (11), the control inputs, denoted by the vector U, are separated from the uncontrolled inputs, denoted by the vector W. The control inputs $U = [U_s \quad U_l \quad U_b]^T$ are the heating flowrates from the space heating system in each zone; the uncontrolled inputs $W = [\phi_{IG_s} \quad \phi_{IG_l} \quad \phi_{IG_b} \quad \phi_{sol} \quad T_{amb} \quad T_g]$ include separately the internal heat gains in each zone, the overall solar incidence radiation on the building surfaces, ambient dry bulb temperature and ground temperature. A set of parameters $[\alpha_1 \quad \alpha_2 \quad \alpha_3]$ are used in the model for each zone as a

coefficient that converts solar radiation into solar gains to each zone. These parameters are included in the parameter matrix to be identified from the data.

$$\dot{x} = A_c\, x + B_c U + E_c W \tag{6}$$

The triplet (A_c, B_c, E_c) is derived through transforming the parameters of the differential equations into a matrix form. It can be seen that only non-variant parameters are included in the three matrices.

$$A_c = \begin{bmatrix} -(\frac{1}{R_4C_1} + \frac{1}{R_1C_1}) & \frac{1}{R_4C_1} & 0 \\ \frac{1}{R_4C_2} & -(\frac{1}{R_4C_2} + \frac{1}{R_2C_2} + \frac{1}{R_5C_2}) & \frac{1}{R_5C_2} \\ 0 & \frac{1}{R_5C_3} & -(\frac{1}{R_3C_3} + \frac{1}{R_5C_3} + \frac{1}{R_6C_3}) \end{bmatrix}$$

$$B_c = \begin{bmatrix} \frac{1}{C_1} & 0 & 0 \\ 0 & \frac{1}{C_2} & 0 \\ 0 & 0 & \frac{1}{C_3} \end{bmatrix} \quad E_c = \begin{bmatrix} \frac{1}{C_1} & 0 & 0 & \frac{\alpha_1}{C_1} & \frac{1}{R_1C_1} & 0 \\ 0 & \frac{1}{C_2} & 0 & \frac{\alpha_2}{C_2} & \frac{1}{R_2C_2} & 0 \\ 0 & 0 & \frac{1}{C_3} & \frac{\alpha_3}{C_3} & \frac{1}{R_3C_3} & \frac{1}{R_6C_3} \end{bmatrix}$$

Parameter estimation

The triplet (A_c, B_c, E_c) includes 12 unknown parameters altogether. They are all physical parameters of the building system; the range of these parameters can, therefore, be estimated a priori. Estimating the parameters using measured or synthetic data is a common practice, where an optimization problem is solved to minimize the prediction errors of the model against the data.

In this study, the synthetic data generated from the detailed model was used for parameter estimation. The measured data was not directly used for this process because it was observed that the measured temperature narrowly swung within the normal operation of HVAC systems, which did not contain enough excitation information for the model to be identified. The measured data, however, as mentioned in the Section *Methodology,* was used to calibrate the detailed model.

The training data was generated using the optimal setpoint profiles proposed by GenOpt, which presented large oscillations (about 7 °C) as can be seen in the later discussions. The period of the data lasts 12 days with a sampling rate of 15 minutes. Each variable, therefore, contains 1152 samples. The defined inputs were ambient dry-bulb temperature, solar radiation and controlled heating flowrates; the outputs (also the system states) were the three zone temperatures. All the

variables were “measured” from the detailed model; no state estimators were therefore designed for the parameter identification process.

After determining the data for the parameter estimation, the next step was to discretize the continuous-state equation in Eq. (6) to a discrete-time form as shown in Eq. (7):

$$x(k+1) = Ax(k) + BU(k) + EW(k) \tag{7}$$

The triplet $(A, B, E) \in R^{3\times3\times6}$ denotes the discretized form of (A_c, B_c, E_c). Using the discretized form, the one- or k-step ahead prediction could be easily formulated. Eq. (8) presents the 1-step ahead estimation of the outputs (or system states). $\hat{x}(k+1)$ represents the estimated system states at time $k+1$, which is a function of the states $x(k)$, the control inputs $U(k)$ and the disturbance inputs $W(k)$ at the time k as well as the parameter matrices (A, B, E). In this prediction, the system states, control inputs and disturbance inputs at the time k are all known; the only unknown parameters are the triplet (A, B, E), or written in a vectorized form as $[R_1 \quad R_2 \quad R_3 \quad R_4 \quad R_5 \quad R_6 \quad C_1 \quad C_2 \quad C_3 \quad \alpha_1 \quad \alpha_2 \quad \alpha_3]$.

$$\hat{x}(k+1) = Ax(k) + BU(k) + EW(k) \quad \text{for} \quad k = 0, 1, \dots, K \dots, N-1 \tag{8}$$

The parameter values were then obtained by minimizing the prediction errors against the synthetic data. The optimization problem of the parameter estimation was formulated in Eq. (9). The optimization algorithm was to find the optimal parameters in the triplet (A, B, E), so that the predicted error from the model was minimized given the information of $x(k)$, $U(k)$ and $W(k)$ for time steps $k = 0,1, \dots, K \dots, N-1$ with N indicating the total number of samples for each variable.

$$J_E = \sum_{k=0}^{N-1} [\hat{x}(k+1) - x(k+1)]^T [\hat{x}(k+1) - x(k+1)] \tag{9}$$

The optimization problem for the prediction error minimization was formulated using the generic nonlinear constrained function “fmincon” from the MATLAB Optimization Toolbox. The algorithm “interior-point” was used, which could converge to an optimal solution within a few minutes.

Model validation

After the model was trained and the values were obtained for the unknown parameters, a new set of data was used to validate the model with the identified parameters. Both 1-step and 1-day (or 96 steps) ahead validations were conducted as shown in Figure 7. It can be seen that the 1-step ahead prediction (shown in the blue curve) was fairly close to the "measured" zone air temperatures for all three zones. Table 3 summarizes the Rooted Mean Square Errors (RMSE) for both 1-step and 1-day model predictions. The 1-step ahead prediction errors for the three zones were all within 0.5 °C. Compared to the 1-step ahead prediction, the 1-day ahead prediction gave slightly worse results with larger errors observed in ten hours later. These are deemed to be acceptable for the control purpose as the model prediction in the MPC controller is updated every 15 minutes.

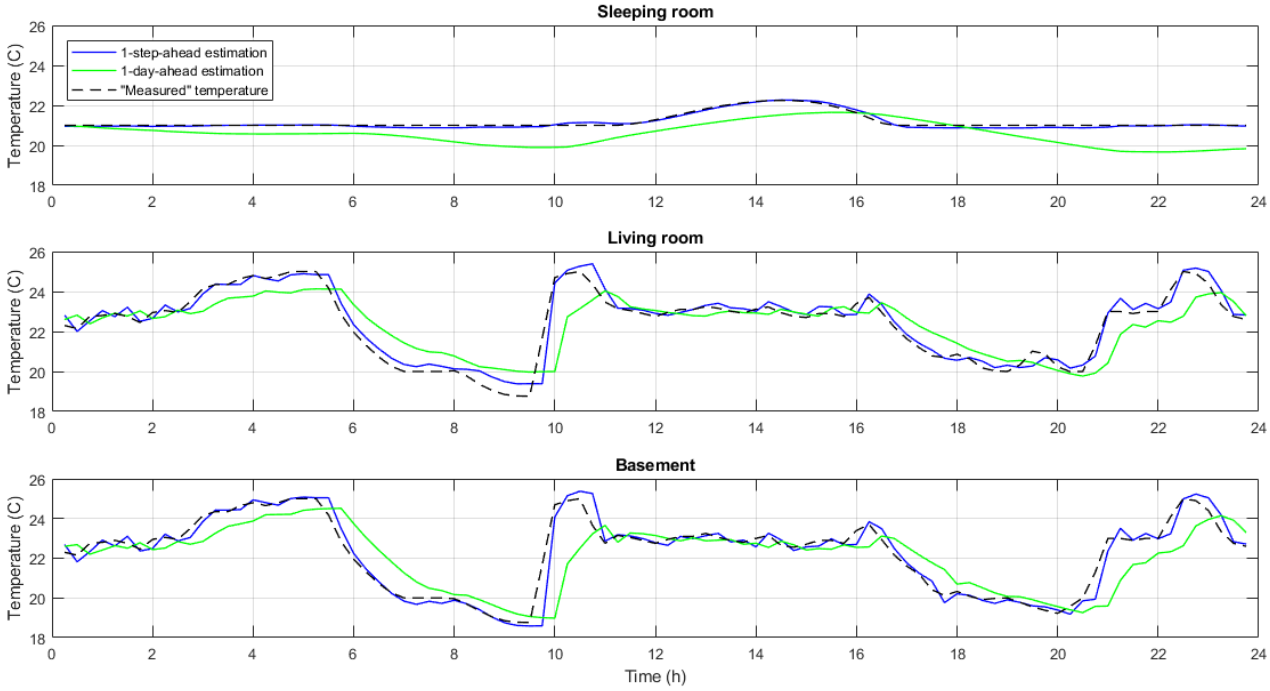

Figure 7: Validation results of the RC model respectively for the Second floor (sleeping room), Main floor (living room) and Basement

Table 3: RMSE results for model validations

	Sleeping room	**Living room**	**Basement**
1-step ahead prediction	0.08 °C	0.4 °C	0.5 °C
1-day ahead prediction	0.7 °C	1.15 °C	2.05 °C

MPC formulation

Once the model has been discretized, it can be straight-forward to formulate the prediction of the outputs (or states) over the prediction horizon as follows:

$$x(k+i+1|k) = Ax(k+i|k) + BU(k+i|k) + EW(k+i|k) \tag{10}$$

P denotes the prediction horizon and i is the sampling interval with $i = 0, 1, \dots, K, \dots, P-1$. $x(k+i|k)$ denotes the predicted states at time interval $k+i$ from sampling instant k. The predicted values for states x (or outputs) and controlled disturbances U are then used to calculate the future control inputs by solving an optimization problem. The goal of the MPC controller is to either increase or decrease power demand during the flexibility events; the objective function can thus be formulated as a function of power cost in the following equation:

$$J(k) = \sum_{i=0}^{P-1} U^T(k+i|k)\, R(k+i)\, U(k+i|k) \tag{11}$$

$U(k+i|k)$, as in both Eq.(10) and (11), denotes the optimal control inputs at time interval $k+i$, while $R(k+i)$, defined as a positive definite matrix, denotes the varying price signal time series. Given the current states $x(k)$ and the predicted disturbances $\{W(k), W(k+1), \dots W(k+P-1)\}$, the objective function $J(k)$ is then minimized subject to a series of constraints. Eq. (12) expresses the constraints in a generic formulation, respectively for the control inputs and states:

$$\begin{cases} G_{eq}x(k+i+1|k) = g_{eq}(k+i) \\ G(k+i)x(k+i+1|k) \le g(k+i) \\ S(k+i)U(k+i|k) \le s(k+i) \end{cases} \tag{12}$$

The first equation is an equality constraint for the states, i.e., zone temperatures. They are the governing equations of the building system. The second is an inequality constraint, which represents the state constraints at each time interval, i.e., the thermal comfort requirement that constraints the zone temperatures in a lower and upper bound. They are a function of time to consider the temperature comfort constraint change from occupied to unoccupied periods. The last inequality is the physical constraints on the inputs, i.e., the minimum and maximum heating capacity. Once the optimization algorithm converged to a solution for the optimal input vector $\{U(k|k), U(k+1|k), \dots, U(k+P-1|k)\}$, the first input signal in the vector is then sent to the local controller. The local controller measures the state variable and compares it with the optimal signal and determines whether to activate the HVAC system. The state measurements are also fed

back to the MPC supervisory controller so that the MPC controller can update its starting states. The feedback loop is thus closed and moves to the next sampling interval and iterates the process.

Results

Simulation studies were conducted to control the space heating system of the CCHT houses using the three control methods as described above. The optimization of the controls lasted only 1 day, which is chosen to have the lowest outdoor dry-bulb temperature from the CWEC weather file for Montreal, Canada (Numerical Logics, 1999). To eliminate the initialization impact of the models, the whole simulation duration was 12 days. In the first 11 days, the zone temperatures were controlled to the reference heating setpoint, so that all methods started from the same initial states of the models.

This section first presents and discusses the time series plots for each control method; then moves on to the quantitative results in terms of the defined KPI metrics.

Time-series results

Figure 8 presents the results of the MPC method using detailed controller models. The DR event durations are denoted by the two vertical bars. The allowable thermal comfort range is shown by the green dashed curves, which has a narrower range when the zone is occupied. The reference setpoints are 21 °C shown by the dashed yellow line and the total reference heating power use is shown by the blue curve. A reference power drop is seen at around 19:00 due to the internal gains from the 8.1 kW dryer and 1.7 kW dishwasher turned on. Power drops at around 7:00 and 17:30 are caused by internal or solar gains in one or more zones. The optimal setpoint profile is shown by the dark dashed curve and the resulted optimal building heating power is shown by the red curve. For the sake of simplicity, only the main floor temperature is shown in the figure. All zone temperatures respect the defined temperature bounds as shown in the figure.

It can be seen that MPC increases the heating setpoint slowly until the maximum temperature limit before the DR events both in the morning and evening. Then it decreases the heating setpoint during the DR events. As a result, the building consumes more electrical energy while the electricity is cheaper; and consumes less electricity while it is more expensive. The pre-bound effect of the MPC method for both DR events is obvious. The rebound effect is however more

pronounced in the afternoon DR event. The morning rebound is almost negligible because the zones are unoccupied after the event. In the evening, the zones have longer occupation time and, in result, longer narrower thermal comfort range. When the afternoon DR event ends, the setpoint increases immediately to heat up the zones because the occupancy time ends 1.5 hours later. Note that the zones are in free-floating mode at around 13:00 and 19:30: the setpoint is decreasing but the zone temperatures do not follow. The setpoint even drifts below the lower bound of temperature limit at around 19:30. This is due to the forecast of solar and internal heat gains in the controller model.

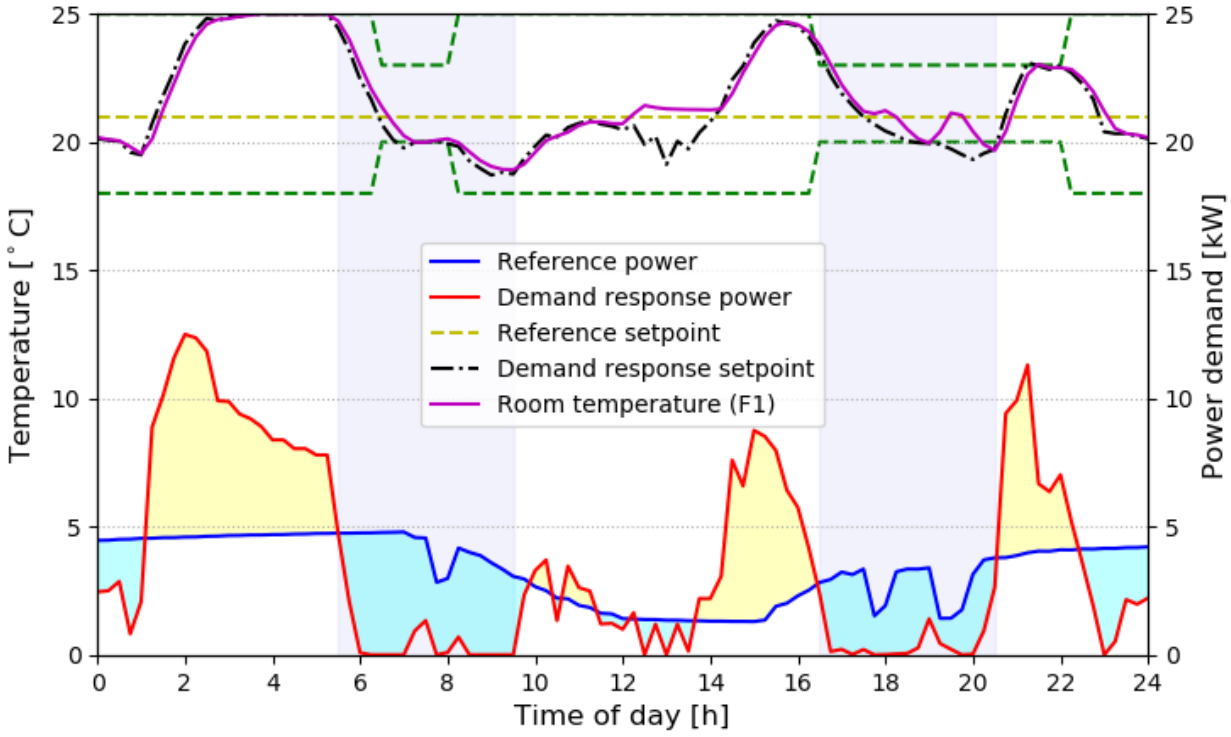

Figure 8: Energy flexibility results using MPC with detailed modelling for the coldest day

In terms of preheating time, it takes about 4 hours in the morning and about 3 hours in the afternoon, which is similar to the 4-hour duration of both DR periods. This shows that the building does not necessarily require a very long preconditioning time, not longer than the DR duration in this case study. When the outdoor temperature is higher and solar radiation is larger in the afternoon, it needs less preheating time for the afternoon DR event.

This MPC method using detailed modelling presents a very effective capability of power shifting in response to the DR events. It can be seen that the heating power demand remains close to zero

for most of the DR durations. This impressive response comes at a cost that the prebound and rebound effects are also quite pronounced.

The results of the MPC method with the reduced-order controller model is presented in Figure 9, which has the same conditions as the MPC method using detailed modelling. The legends of the figure are consistent with that in Figure 8. A similar pattern of the optimal setpoint profile is observed: MPC slowly ramps up the heating setpoint before the DR events and drops the setpoint during the events. As a result, the heating system uses more electrical power before the events and less power during the events. The difference of this MPC method is that it does not increase the zone temperatures to the maximum allowed limit, leaving a safety margin to the thermal constraints. As a result, the preheating effect is less aggressive than the MPC method with the detailed controller model. The reduced power use against the reference profile during the DR events is thus not as significant. Similarly, the prebound and rebound energy use is not as high either. Given that this MPC method uses a reduced-order controller model, it unavoidably presents prediction errors of the "real system". This is different from the MPC method with the detailed controller model, which assumes perfect modelling of the real system and represents a best-case scenario for the optimization algorithm.

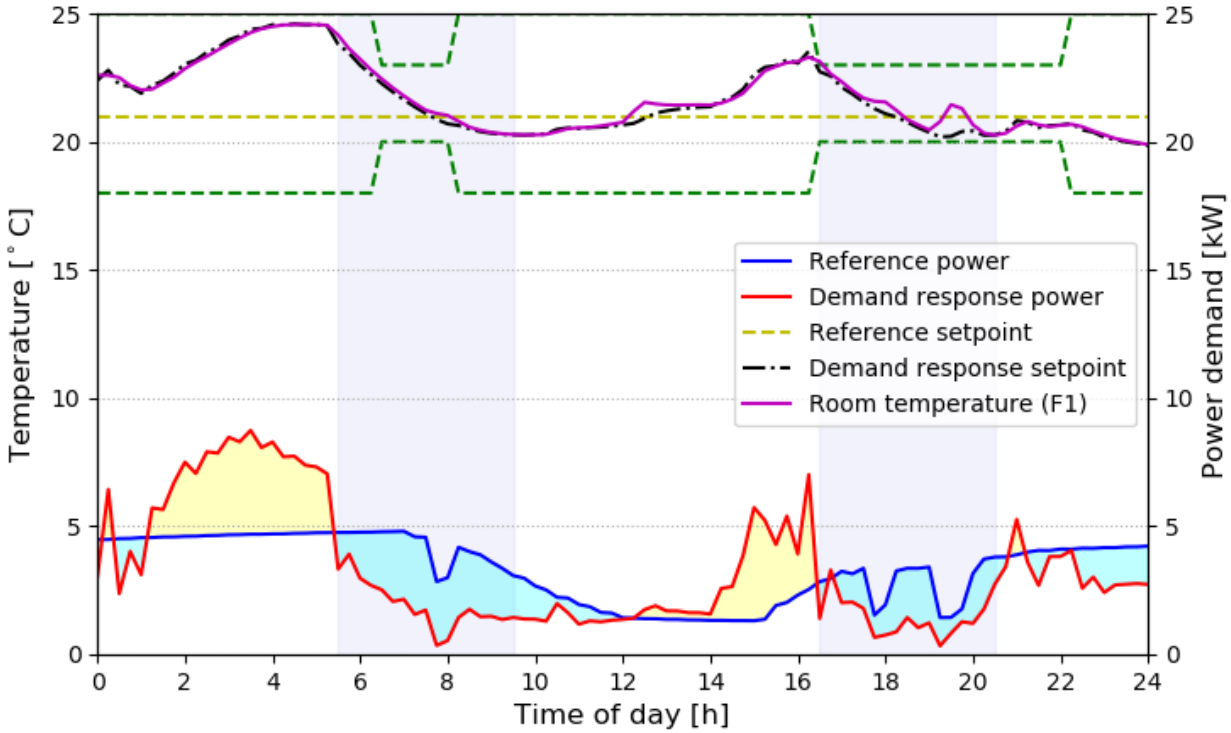

Figure 9: Energy flexibility results using MPC with the reduced-order model for the coldest day

Compared with the reference case, the MPC with the reduced-order controller model still presents significant power reductions during the DR periods. The prebound phenomena are also obvious but the rebound effect is almost negligible for both DR events. After the end of the afternoon DR event, the MPC decides to slightly increase the heating setpoint, which is a better decision than that proposed by the MPC method with detailed modelling. The main advantage of the MPC method with the reduced-order model is its computation time: it took about only 20 seconds for the whole simulation duration: 12-day simulation with 1-day optimization, which is in the same order as the reference case. The MPC method with the detailed modelling, however, took about 16.3 hours for the simulation-optimization task, where most of the time was spent for the 1-day optimization.

The simulation results of the RBC strategy under the same conditions are shown in Figure 10. The proposed reactive heuristic algorithm is described as below: before the morning DR event, keep the setpoint temperatures at the reference setpoint; decrease the setpoints by 1 °C from 5:30 to 8:30; decrease the setpoints further by 2 °C to the new lower temperature bound until 9:30; reset the setpoints back to the reference setpoint and decrease the setpoints by 1 °C for the whole afternoon DR period. This heuristic setpoint algorithm is chosen because it is probably one of the best reactive strategies given the same conditions and constraints from the MPC methods. For example, the setpoint drop from 5:30 to 6:30 was determined to be 1 °C instead of 2 °C or more until the lower temperature bound because a 2 °C setpoint drop resulted in a larger power increase than the reference case at 6:30 in the simulation. It required a large heating power when the setpoint was reset to 20 °C, the lower temperature bound during the occupied period. This thus presented to be a bad strategy with a power rebound during the DR period.

The resulting power demand profile of RBC shows that the immediate power reduction is quite significant, which goes almost to zero in the morning and reaches zero in the afternoon. The power has to increase due to the thermal comfort constraints, but it is never higher than the reference case. The rebound effect occurs only after the end of the DR events due to its reactive nature and the rebound effect is also quite significant, especially for the morning DR event.

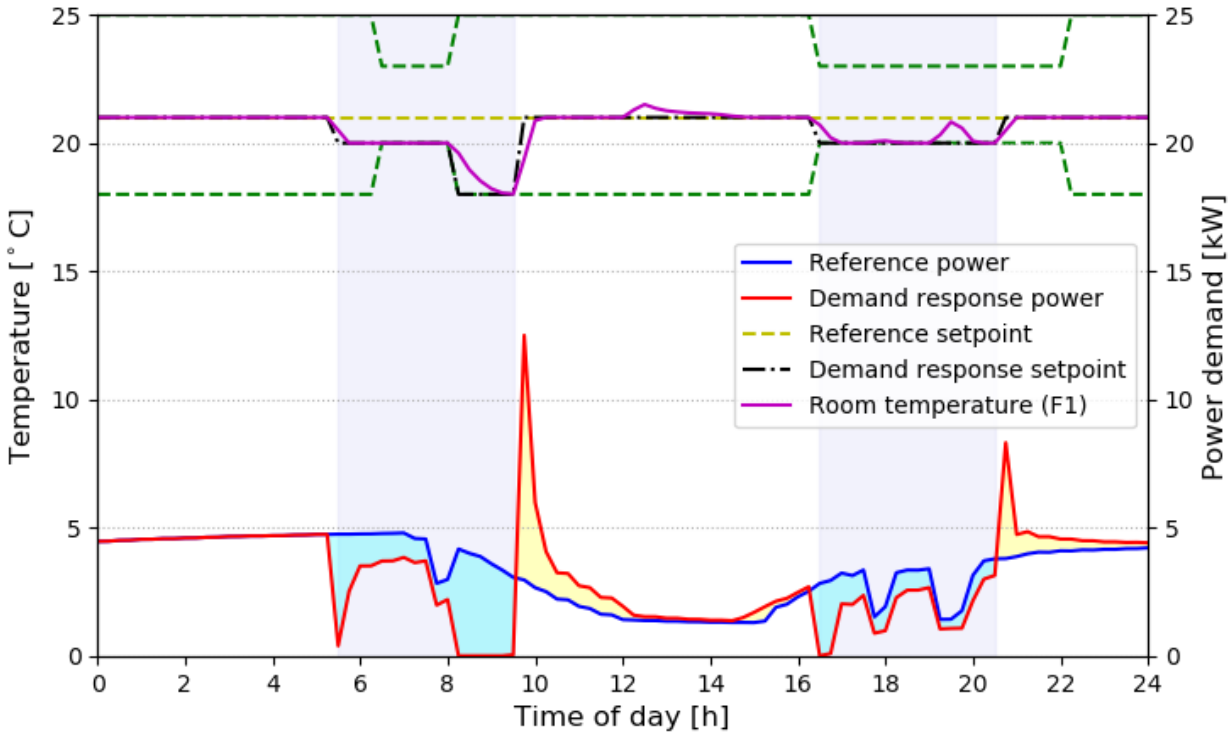

Figure 10: Energy flexibility results using rule-based control strategy for the coldest day

KPI results

Table 4 summarizes the results of the two MPC approaches and the RBC strategy using the KPI metrics. It can be seen that both MPC methods deliver very impressive flexible energy during the DR periods. The MPC methods also result in large pre-bound and rebound energy as shown in the fourth row. Their flexible efficiencies are less than 1 because the total rebound energy is larger than the flexible energy for both methods. The maximum flexible powers using the MPC methods almost reach the maximum potential in the morning DR event.

The method with the reduced-order model presents less flexible energy than the one with the detailed model. The former, however, shows with less rebound effect. The flexible efficiency of the former method thus is higher than with that of the latter, especially in the afternoon event. The maximum flexible power of the former method is comparably significant to that of the latter. This result difference validates that the accuracy of the controller model has a large impact on the results of the MPC formulation.

Comparing the RBC method with the two MPC methods, both MPC methods provide much larger flexible energy than RBC, especially in the afternoon event. The MPC method with the detailed

controller model presents more than twice flexible energy than RBC in the morning event and more than three times flexible energy in the afternoon event. And this comparison is reasonable because the RBC algorithm represents a best-case reactive controller as mentioned previously.

Table 4: Summary of energy flexibility indicators for MPC and RBC

	Morning event			**Afternoon event**		
	MPC (detailed)	MPC (reduced order)	RBC	MPC (detailed)	MPC (reduced order)	RBC
Flexible energy [kWh]	15.1	9.1	7.3	9.5	5.4	3.7
Rebound energy [kWh]	21.0	11.7	4.7	18.2	6.8	2.6
Flexible efficiency [-]	0.72	0.78	1.55	0.52	0.79	1.4
Max flexible power [kW]	4.8	4.5	4.0	3.3	2.8	2.8

The MPC methods also have larger maximum flexible power than RBC, but their differences are not as significant because all methods show very good power reduction capabilities against the reference case. The MPC with the detailed model presents about 20% more maximum flexible power than RBC; the MPC with the reduced-order model presents about 8% more maximum flexible power than RBC. The cost of the MPC methods is their more-obvious rebound effect than RBC. Both MPC methods present larger rebound energy use than their flexible energy, while the RBC presents less rebound energy than its flexible energy. As a result, RBC has an efficiency larger than 1 while the MPC methods have an efficiency smaller than 1.

From the above discussions, it can be seen that no one approach presents absolute advantages than the other using the four indicators. In other words, it cannot be concluded that the MPC strategy is a more suitable approach than the RBC strategy to increase the building energy flexibility, at least not for this case study. If the objective of the building operation is to provide as much flexible energy as possible, MPC is shown to be a better candidate if the cost of hardware installation and software deployment associated with MPC is justifiable. If the objective is to increase the flexibility efficiency, then a fined-tuned RBC strategy is more advantageous.

Conclusions

Buildings can be operated in an energy-flexible manner while respecting occupant requirements of indoor thermal comfort. This energy flexibility, both in time and quantity, can be harnessed by the electrical grid to balance its supply and demand. In the context of smart grid and intelligent buildings, the concept of energy flexibility in buildings broadens the existing demand management thinking from the top-down one-way control to two-way communications. This energy flexibility of buildings can be generally viewed in two scenarios: upward and downward flexibility. The upward flexibility represents scenarios of increasing building demand during the DR events, while the downward flexibility represents scenarios of decreasing building demand during the events. The conventional grid services such as demand limiting, load shedding, load shifting, load tracking can be regarded as either downward flexibility, or a combination of downward and upward flexibility at a given time period."

To quantify the flexibility from this new perspective, the paper introduced four indicators, two of them adapted from existing literature and two others proposed by the authors. Based on the metrics, the paper investigated two different control methods, MPC and RBC, and evaluated their performances accordingly. Specifically, the MPC strategy was implemented in two different approaches: one with a detailed building model in the controller; the other with a reduced-order controller model. The former MPC, implemented using co-simulation between TRNSYS and GenOpt, represents the best MPC potential due to no modelling errors. The latter, implemented using co-simulation between TRNSYS and MATLAB, represents a more realistic implementation that can be deployed in a thermostat with limited computational power. Both MPC and RBC methods were simulated in a feedback control loop with an idealized local controller. The RBC algorithm was implemented based on the best heuristic rules, subject to the same occupancy and thermal comfort constraints of the two MPC methods.

Simulation results showed that both MPC implementations delivered significantly more potential for energy flexibility than the RBC strategy. The MPC approach using the detailed controller model provided two to three times of flexible energy than that of the RBC strategy during the DR events. The MPC approach using the reduced-order controller model, even though less impressive than the former MPC method, also showed about 30% more flexible energy than RBC. The MPC method with the detailed model takes about 16 hours to finish a 24-hour simulation, while the

MPC method with the reduced-order model finishes the same duration of simulation within 1 minute, in the same magnitude as the RBC method. On the other hand, the RBC method showed much less rebound energy; its flexible efficiency is about twice of that of the MPC methods. For the maximum flexible power, the MPC methods presented 8% to 20% more potential to change the power during the DR events than the RBC method.

In terms of implementation effort, the RBC strategy is the easiest to implement and deploy on a real controller. The RBC algorithm is also more stable and reliable. In contrast, the MPC methods suffer high implementation costs and difficulty for scalability. For the reduced-order controller model, identifying a suitable model for real-world deployment is probably one of the biggest obstacles for MPC applications. The MPC strategy is also subject to a variable of uncertainties, for instance, the difficulty of modelling internal gains accurately, which may reduce its performance and usability.

The limitation of the paper includes that the local thermostat was modelled as an idealized controller. A realistic PID controller may show different response curves that change the results based on the proposed indicators. The choice of the RBC algorithm is also critical when comparing with MPC. An RBC method with a pre-conditioning algorithm may show very different results.

Future studies of the work could include:

- Because the MPC configuration with detailed modelling is rather computationally-intensive, only a one-day simulation period was investigated in the current work. A longer period of optimization-simulation could be conducted to assess the MPC methods under different climate conditions. A statistical analysis based on the whole-year simulation could be carried out further to investigate the overall differences between the two control strategies.
- Only one building was simulated for the case study. The amount of building energy flexibility would be more significant if we apply the same method on a larger scale, e.g., a cluster of buildings or district energy systems.
- Buildings of other types such as commercial and institutional buildings could also be investigated using the method detailed in this work to characterize their potential of energy flexibility.

- For the MPC strategy, assumptions of perfect forecasting were made for internal gains, occupancy and weather. The impact of imperfect disturbance forecast could be investigated and a field study of the developed MPC strategy could be conducted to further test the effectiveness of the method.
- The thermal comfort in the MPC formulation is defined as either a hard or soft constraint. If considering thermal comfort improvement as another objective, a multi-objective function could be defined for the MPC problem, which maximizes both energy flexibility and thermal comfort. In this case, a new indicator would be necessary to evaluate the thermal comfort changes; or to evaluate the weighted effect of both thermal comfort and energy flexibility at the same time.

References

Alstone, P., Potter, J., Piette, M. A., Schwartz, P., Berger, M. A., Dunn, L. N., … Jain, A. (2017). *2025 California Demand Response Potential Study - Charting California's Demand Response Future. Final Report on Phase 2 Results*. https://doi.org/10.2172/1421800

Bacher, P., & Madsen, H. (2011). Identifying suitable models for the heat dynamics of buildings. *Energy and Buildings*, *43*(7), 1511–1522. https://doi.org/10.1016/j.enbuild.2011.02.005

Barzegar, B., Zhang, K., & Kummert, M. (2018). Energy flexibility analysis for photovoltaic solar system with battery. *Proceedings of ESim 2018, May 9-10, 2018*, 183–192.

California ISO. (2017). *Impacts of renewable energy on grid operations*. Retrieved from https://www.caiso.com/Documents/CurtailmentFastFacts.pdf

Davito, B., Tai, H., & Uhlaner, R. (2010). *The smart grid and the promise of demand-side management*. Retrieved from http://www.calmac.com/documents/MoSG_DSM_VF.pdf

De Coninck, R., & Helsen, L. (2016). Quantification of flexibility in buildings by cost curves - Methodology and application. *Applied Energy*, *162*, 653–665. https://doi.org/10.1016/j.apenergy.2015.10.114

Finck, C., Clauß, J., Vogler-Finck, P., Beagon, P., Zhang, K., & Kazmi, H. (2018). *Review of applied and tested control possibilities for energy flexibility in buildings Review of applied and tested control possibilities for energy flexibility in buildings*. https://doi.org/10.13140/RG.2.2.28740.73609

Jensen, S. Ø., Henrik, M., Lopes, R., Junker, R. G., Aelenei, D., Li, R., … Pasut, W. (2017). Annex

67: Energy Flexible Buildings - Energy Flexibility as a key asset in a smart building future. Retrieved from http://annex67.org/media/1470/position-paper-energy-flexibility-as-a-key-asset-i-a-smart-building-future.pdf

Jensen, S. Ø., Marszal-Pomianowska, A., Lollini, R., Pasut, W., Knotzer, A., Engelmann, P., … Reynders, G. (2017). IEA EBC Annex 67 Energy Flexible Buildings. *Energy and Buildings*, *155*, 25–34. https://doi.org/10.1016/j.enbuild.2017.08.044

Karnouskos, S., Ilic, D., & Silva, P. G. Da. (2012). Using flexible energy infrastructures for demand response in a Smart Grid city. *IEEE PES Innovative Smart Grid Technologies Conference Europe*, 1–7. https://doi.org/10.1109/ISGTEurope.2012.6465859

Kathirgamanathan, A., Péan, T., Zhang, K., Rosa, M. De, Salom, J., Kummert, M., & Finn, D. P. (2020). Towards Standardising Market-Independent Indicators for Quantifying Energy Flexibility in Buildings. *Energy and Buildings*, 110027. https://doi.org/10.1016/J.ENBUILD.2020.110027

Le Dréau, J., & Heiselberg, P. (2016). Energy flexibility of residential buildings using short term heat storage in the thermal mass. *Energy*, *111*(1), 1–5. https://doi.org/10.1016/j.energy.2016.05.076

Li, R., Dane, G., Finck, C., & Zeiler, W. (2017). Are building users prepared for energy flexible buildings? A large-scale survey in the Netherlands. *Applied Energy*, *203*, 623–634. https://doi.org/10.1016/j.apenergy.2017.06.067

Manning, M. M., Swinton, M. C., Szadkowski, F., Gusdorf, J., & Ruest, K. (2007). The Effects of thermostat setting on seasonal energy consumption at the CCHT Twin House Facility. *ASHRAE Transactions*, *113*(1), 1–12.

Mathews, E. H., Richards, P. G., & Lombard, C. (1994). A first-order thermal model for building design. *Energy and Buildings*, (21), 133–145. https://doi.org/10.1016/0378-7788(94)90006-X

Natural Resources Canada. (2012). *2012 R-2000 Standard*. Ottawa, ON: Natural Resources Canada's Office of Energy Efficiency.

New Buildings Institute. (2018). The GridOptimal Initiative. Retrieved August 17, 2018, from https://newbuildings.org/wp-content/uploads/2018/01/NBI_USGBC_GridOptimalInitiative010918_PresentationSlides.pdf

Nuekomm, M., Nubbe, V., & Fares, R. (2019). *Grid-interactive Efficient Buildings: Overview*.

Numerical Logics. (1999). *Canadian Weather for Energy Calculations, User's Manual and CD-ROM*. Downsview, Ontario: Environment Canada.

Palensky, P., & Dietrich, D. (2011). Demand side management: Demand response, intelligent energy systems, and smart loads. *IEEE Transactions on Industrial Informatics*, *7*(3), 381–388. https://doi.org/10.1109/TII.2011.2158841

Quintana, H. J., & Kummert, M. M. (2015). Optimized control strategies for solar district heating systems. *Journal of Building Performance Simulation*, *8*(2), 79–96. https://doi.org/10.1080/19401493.2013.876448

Reynders, G., Diriken, J., & Saelens, D. (2015). A generic quantification method for the active demand response potential of structural storage in buildings. *14th International Conference of the International Building Performance Simulation Association (IBPSA), Hyderabad, India, Dec. 7-9, 2015*, 1986–1993.

Reynders, G., Diriken, J., & Saelens, D. (2017). Generic characterization method for energy flexibility: Applied to structural thermal storage in residential buildings. *Applied Energy*, *198*, 192–202. https://doi.org/10.1016/j.apenergy.2017.04.061

Rodríguez Jara, E., Sánchez de la Flor, F. J., Álvarez Domínguez, S., Molina Félix, J. L., & Salmerón Lissén, J. M. (2016). A new analytical approach for simplified thermal modelling of buildings: Self-Adjusting RC-network model. *Energy and Buildings*, *130*, 85–97. https://doi.org/10.1016/j.enbuild.2016.08.039

Ulbig, A., Borsche, T. S., & Andersson, G. (2014). Impact of low rotational inertia on power system stability and operation. *IFAC Proceedings Volumes (IFAC-PapersOnline)*, *19*, 7290–7297. https://doi.org/10.3182/20140824-6-ZA-1003.02615

Yin, R., Kara, E. C., Li, Y., DeForest, N., Wang, K., Yong, T., & Stadler, M. (2016). Quantifying flexibility of commercial and residential loads for demand response using setpoint changes. *Applied Energy*, *177*, 149–164. https://doi.org/10.1016/j.apenergy.2016.05.090

Zhang, K. (2018). *Model Predictive Control of Building Systems for Energy Flexibility* (Polypublie Polytechnique Montreal). Retrieved from https://publications.polymtl.ca/3550/1/2018_KunZhang.pdf

Zhang, K., & Kummert, M. (2018). Potential of building thermal mass for energy flexibility in residential buildings: a sensitivity analysis. *Proceedings of ESim 2018, May 9-10, 2018*, 163–172.